Solid State Science and Technology, Vol. 18, No 1 (2010) 288-301
ISSN 0128-7389

VIBRATIONAL STUDIES OF CRYSTALLINE PHASE STRONTIUM MAGNESIUM PHOSPHATES DOPED WITH Eu_2O_3

Rosli Hussin[1], Muhammad Shawal Husin[1], Dayang Nur Fazliana Abdul Halim[1] and Sinin Hamdan[2]

[1]*Phosphor Research Group, Department of Physics, Faculty of Science, Universiti Teknologi Malaysia, Skudai, 81310, Johor*

[2]*Department of Mechanical and Manufacturing System, Faculty of Engineering, Universiti Malaysia Sarawak, 94300, Kota Samarahan, Sarawak*

ABSTRACT

In order to verify the assignments of the vibration modes and to find correlations in the changes induced by Eu_2O_3 in strontium magnesium phosphate with the composition of $27.5SrO\text{-}27.5MgO\text{-}45P_2O_5$ as phosphor host matrix was prepared and investigated using Raman and Infrared (IR) spectroscopy. The doping concentration of Eu_2O_3 ions were varies from 1-5 mol%. The results of this study shows that Raman spectroscopy was give better structure change comparable to IR spectroscopy. Raman spectra of the studied sample present the specific bands of the phosphate network when doping with Eu_2O_3 ions, but structural change in IR spectra is unnoticeable, due to a characteristic of symmetry materials. The position of most Raman and IR bands do not coincide indicating a higher symmetry. The characteristics features of $27.5SrO\text{-}27.5MgO\text{-}45P_2O_5$ undoped spectrum are the PO_2 asymmetric stretching vibration band at 1240 cm^{-1}, $\nu_{as}(PO_2)$, the PO_2 symmetric stretching vibration band at 1171 cm^{-1}, $\nu_s(PO_2)$, the $\nu_{as}(PO_3)$ groups (chain-end groups) at 1136 cm^{-1}, the ν_s of PO_3 groups near 1062 cm^{-1}, the ν_{as} of POP groups at 900 cm^{-1}, the ν_s of POP groups at 780 and 688 cm^{-1} and the deformation modes of $P\text{–}O^{-}(PO_4^{3-})$ groups at 562 and 477 cm^{-1}. The crystallized phases obtained with high doping Eu_2O_3, exhibited the Raman bands related to the orthophosphate (Q^0) structure along with the pyrophosphate (Q^1), and traces of metaphosphate (Q^2) units. Based on stoichiometric, only Q^1 and Q^2 units were expected to be present, but the Raman spectra indicated detectable concentration of Q^0 units, which results from disproportion reactions that occur during the reorganization of the powder sample.

INTRODUCTION

Recent technological applications have generated more interest in the studies of glass or glass ceramic materials. These materials doped with rare earth active ions find a place in the phosphor and luminescence materials application, such as has been used as lamp phosphors, cathode ray tube phosphors and scintillator phosphors, because of their unique spectroscopic properties [1, 2]. New hosts doped with rare earth ions are getting much attention owing to their potential applications.

Among composition glasses or glass ceramic oxide systems, phosphate based are

Corresponding Author: rbh@dfiz2.fs.utm.my

particularly attractive hosts because they can accommodate large concentrations of active ions without losing the useful properties of the material due to their several special properties such as large thermal expansion coefficients, low melting temperatures, solubility etc. In addition, the phosphate systems are relatively easy to prepare and offer an important range of compositional possibilities, which facilitate tailoring of the physical and chemical properties of interest for specific technological applications. The considerable variety in crystal structure of the phosphate compounds provides a great deal of objects for the study aiming at exploring new functional materials. However, the detailed studies concerned with the structure and properties of phosphate glasses have been rather limited due to the hygroscopic behavior of phosphate system and the volatility of P_2O_5 at elevated temperatures [3]. One approach to increasing the chemical durability is to add various oxides to phosphate glasses, such as SnO, PbO, ZnO, Al_2O_3 and Fe_2O_3, etc. These oxides lead to the formation of Sn–O–P, Pb–O–P, Zn–O–P, Al–O–P and Fe–O–P bonds which replace the easily hydrolysable P–O–P bonds and improve dramatically the chemical durability of the modified phosphate glasses [4–11]. A second alternative of improving the chemical durability of phosphate glasses is to replace part of oxygen atoms by nitrogen [9].

The developments of phosphate based materials for a variety of technological applications, from rare-earth ion hosts for solid state lasers to low temperature sealing glasses, have led to renewed interest in understanding the structures of these unusual materials. Subsequent interest in alkaline earth phosphate system as examples, stemmed from their high transparency for ultraviolet (UV) light, when compared with silicate based. As far as luminescence is concerned, attention has been brought to alkaline earth phosphate lattices doped with rare earth ions, because it has high luminescence, moderately synthetically temperature, great X color coordinate and low thermal degradation.

Vibrational spectroscopy gives a lot of information about materials structure. In the case of ionic-molecular structures (for example silicates, phosphates, borates, etc.) spectra interpretation is very difficult because of the influence of the crystalline field on molecules, lattice point interactions and changing the free translations and rotations in molecules into additional vibrations in a crystal [3, 12-17]. These difficulties can be partly eliminated through the parallel use of two complementary spectroscopic methods: Raman and Infrared spectroscopy [17].

The structural characterization is important because it has been shown that the host material of the phosphor phosphates depend onto their chemical and physical stability which are intimately related to their structure and composition in the phosphate range. This work is a part of our ongoing program to synthesis suitable host phosphor with desirable properties; therefore, an understanding of the structure will help shed light on the relationship between structure and luminescent properties, which could expand their applications. In this paper, we explore the complimentarily technique of X-ray diffraction for medium/long-range order studies and vibration spectroscopy (Infrared and Raman) as important tools to provide short range structural information about

Corresponding Author: rbh@dfiz2.fs.utm.my

phosphate system. The aim of this paper is to obtain valuable information concerning a relationship between meta-pyro-phosphate composition, host structure and crystalline phase present in this system, which has a potential candidate for use in powder phosphor material.

In the present paper the structural units constituting the phosphate networks were classified by the Q^n notation where n (n = 0, 1, 2, 3) is the number of bridging oxygen in a PO_4 group. The networks of phosphate can be classified by oxygen-to-phosphorus ratio, which sets the number of tetrahedral linkages, through bridging oxygen, between neighboring P-tetrahedral [18]. In condensed phosphates, three main building groups exist, which are the Q^1 or end unit, the Q^2 or middle unit and the Q^3 or branching unit. Isolated orthophosphate groups are accordingly denoted as Q^0 groups. The PO_4 tetrahedron can be attached to a maximum of three neighboring tetrahedral forming a three-dimensional network as in vitreous P_2O_5 [18,19,20].

EXPERIMENTAL

A nominal composition of powder sample 27.5SrO-27.5MgO-45P_2O_5 doped with Eu_2O_3 (1-5mol%) were prepared using solid state reaction. The batch mixture (20g) was prepared using raw materials of reagent grade $SrCO_3$, MgO and H_3PO_4 (85%). The corresponding weights of the starting materials were mixed thoroughly in alumina crucible and placed in an electric furnace in air. A three-step melting schedule was employed to minimize volatilization losses of low-melting starting materials as well as to ensure homogeneous mixing of the constituents. At the first step, the temperature was set to 100 ^oC with heating rate of 5.0 ^oC/min, and maintained for 1 h to facilitate evaporation of water released by H_3PO_4. The temperature was then raised to 300 ^oC (heating rate 20 ^oC/min) and left for about 1 h in order to evaporate carbonate and water in the batch, and minimize the tendency of subsequent phosphate loss. In the third step, the temperature was increased slowly to 900–1250 ^oC with heating rate of 10 ^oC/min and kept there for 2 h in air.

The structure of the crystalline and amorphous prepared samples was analyzed by means of X-ray diffraction measurements (XRD), using powders form. The XRD measurements were carried out with CuK_α radiation operating at 40 kV, 30 mA with Bragg–Brentano geometry at room temperature using Siemens Diffractometer D5000, equipped with diffraction software analysis. Diffraction patterns were collected in the 2θ range from 10 to 70^o, in steps of 0.04^o and 4s counting time per step.

FTIR spectra were recorded with a Perkin-Elmer (Spectrum One FT-IR spectrometer) in the frequency range 400-4000 cm^{-1} at room temperature. Pellets were prepared for FTIR measurements by mixing and grinding a small quantity of powder sample with spectroscopic grade dry KBr powder and then compressing the mixtures to form pellets for measurements. All measurements were at 4 cm^{-1} resolution and 100 scans.

The Raman spectra were measured with a Perkin–Elmer (Spectrum model 2000R NIR

Corresponding Author: rbh@dfiz2.fs.utm.my

FT-Raman spectrometer) in the spectral range 100–4000 cm^{-1}, with the laser power on the samples being 250 mW. The spectrometer uses an ytterbium aluminum garnet crystal doped with triply-ionized neodymium (Nd:YAG) as a lasing medium. The laser is software-controlled, diode-pumped running at 810 nm, with power of 1600 mW or 750 mW TEM00 and typical working power range from 100 mW to 1 W. The resultant Gaussian beam profile is vertically polarized to better than 100:1. The amplitude stability is better than 0.1 rms and is controlled by means of active optical feedback. The laser line width gives a spectral resolution of better than 0.5 cm^{-1}.

RESULTS AND DISCUSSION

Fig.1 shows the X-ray diffraction patterns (XRD) of crystallized powder compounds with composition 27.5SrO-27.5MgO-45P_2O_5 doped with Eu_2O_3, follow to the standard card of orthorhombic α- $Sr_2P_2O_7$ (JCPDS no. 24-1011), monoclinic MgP_2O_7 (JCPDS no. 27-1273). For the α- $Sr_2P_2O_7$, all the XRD lines match the lines given in no. 24-1011 of JCPDS data files. It can be found that the structure of the powder is in pure orthorhombic phase (α- $Sr_2P_2O_7$). The unit cell parameters obtained are a =8.917A˚, b = 13.16A˚, c = 5.400A˚, respectively. The structure of MgP_2O_7 is in pure monoclinic phase, which is similar to that reported for the compound MgP_2O_7 (JCPDS no. 27-1273). As for the powder samples, the results indicate that there exist the mixed phases of the α-$Sr_2P_2O_7$ and MgP_2O_7 in the samples, as shown in Figure 1.

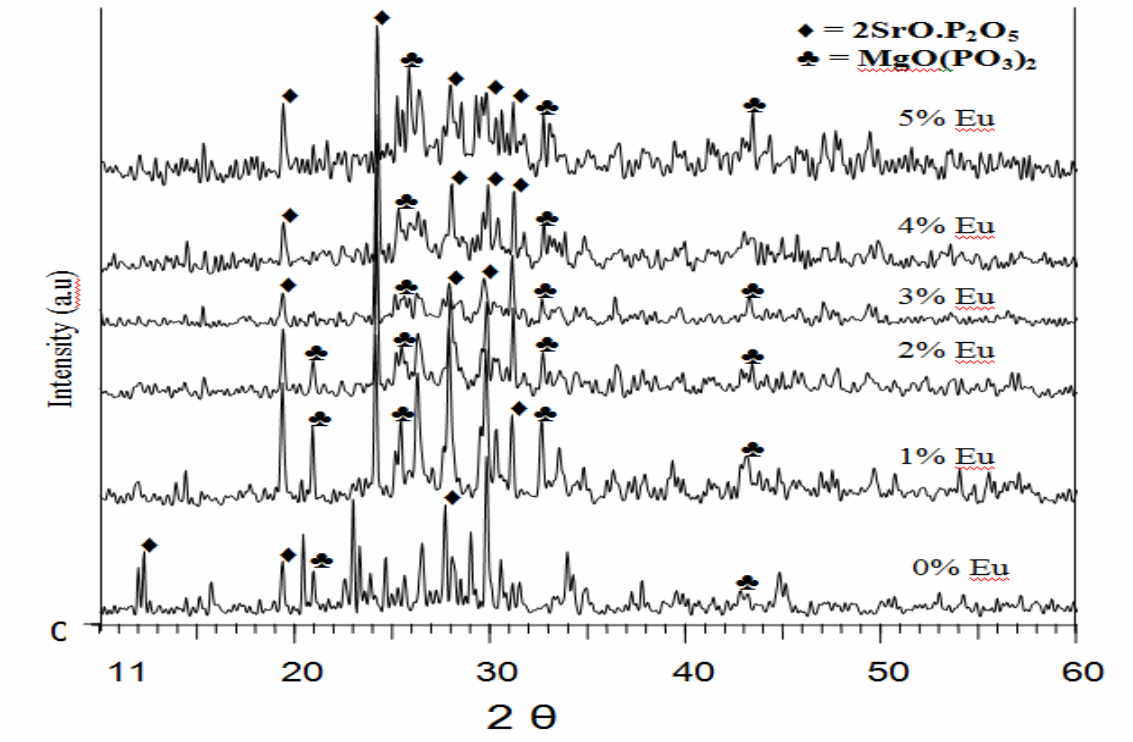

Figure 1. XRD patterns of 27.5SrO-27.5MgO-45P_2O_5: Eu_2O_3 (1-5 mol%)

Corresponding Author: rbh@dfiz2.fs.utm.my

Solid State Science and Technology, Vol. 18, No 1 (2010) 288-301
ISSN 0128-7389

FT-IR spectra of the studied powder sample 27.5SrO-27.5MgO-45P_2O_5: xEu_2O_3 ($1 \leq x \leq 5$ mol %) in the frequency range 400–1400 cm^{-1} is shown in Figure 2. The IR bands are assigned based on the literature data on the wave number ranges related to the corresponding vibrations of the structural units in various glassy and crystalline phosphates [21–23]. Due to two crystalline phase present in the sample, the IR and Raman spectra obtain are very complex and the factor group approach has not been used to the interpretation of the powder spectra. The analysis in the previous papers of the measured spectra was generally made on the basis of characteristic vibrations of the PO_2 terminal and POP bridging units [3,17]. The most important bands and their assignments are given in Table 1.

The bands arising from the vibrations of the phosphate network appear in the range 1400–500 cm^{-1}. Three main regions can be distinguished in this range: the region between 1400–1150 cm^{-1} is characteristic of vibrations of non-bridging (PO_2) groups, the region around 1150–900 cm^{-1} is characteristic of terminal P–O^- and PO_3 groups, and the region between 900 and 700 cm^{-1} is characteristic of the vibrations of bridging (P–O–P) groups. All the symmetric and asymmetric stretching vibrations observed in the spectra are characteristic of Q^1 and Q^2 groups.

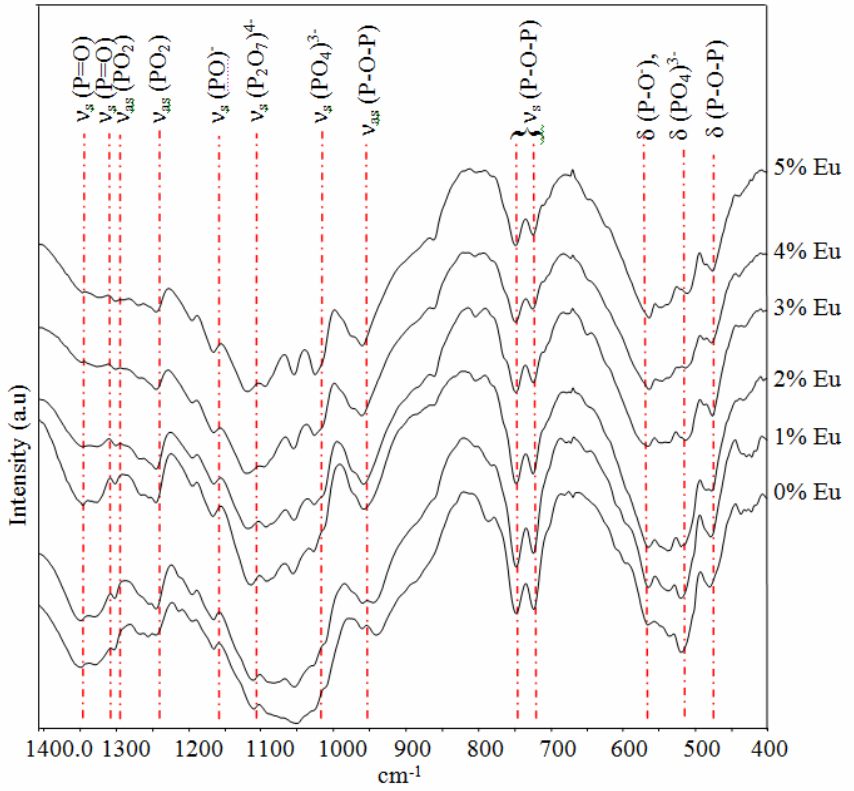

Figure 2: FT-Infrared spectra of powder samples 27.5SrO-27.5MgO-45P_2O_5: xEu_2O_3

Table 1: Raman and IR vibrational modes for 27.5SrO-27.5MgO-45P_2O_5:Eu^{2+} and

Corresponding Author: rbh@dfiz2.fs.utm.my

comparison with the reported values for phosphate system (glass and crystalline).

Reported Value	**Vibrational mode**	**Assignments**	**Observed in this work Wavenumber (cm^{-1})**	
			IR	Raman
3300	ν_s(O-H)	Symmetric stretching of O-H groups	3447s	3400
2900	ν (P-O–H)	Stretching vibrations of the P–O–H group in different structural sites.	2925vw	-
1630	$\delta(H_2O)$	Deformation modes of OH group, absorbed water molecules	1637w 1440w	-
1380 1320 1270	ν (P=O)	Symmetric stretching mode of P=O	1344m 1323w	1350w 1322s 1290s
1200-1340	$\nu_{as}(PO_2)$	Asymmetric stretching mode of the two nonbridging oxygen atoms bonded to phosphorus atoms,the O-P-O or $(PO_2)_{as}$ units, in the phosphate tetrahedral, in Q^2 species	1297-1240m	1240vw
1100–1180	$\nu_s(PO_2)$	PO_2 symmetric stretching vibrations in O–P–O groups of corner sharing PO_4 tetrahedra, Q^2 species	1190m	1171vs
1090-1120	ν (P-O) $\nu_s(PO_3)^-$	Overlap several modes PO_3 terminal/end group and PO_2 middle group/ $P\text{-}O^-$ chain terminal groups/ Q^1 chain terminator	1162m	1136vs
1000-1130	$\nu_s(PO_3)^{2-}$ $\nu(P_2O_7)^{4-}$	Vibrations of terminal / end groups PO_3, Q^1 species	1107m	1072m 1062m
1030	$\nu_s(PO_4)^{3-}$	Symmetric stretching modes of P-non bridging (or terminal) bonds, Q^1 chain terminator	1023sh	967m
900-1100 855-938 700 – 900 705–750	ν_{as}(P–O–P)	Asymmetric stretching bridging oxygen atoms bonded to a phosphorus atom, P–O–P groups in a Q^2 phosphate tetrahedron	958m	900vw
742	ν_s(P–O–P)	The bridging (P–O–P) oxygen atoms in Q^1 phosphate groups	-	730-780-w
720-810	ν_s(P–O–	Symmetric stretching modes of	721-	688vs

Corresponding Author: rbh@dfiz2.fs.utm.my

620-820	P)	bridging oxygens atoms bonded to a phosphorus atom in a Q^2 phosphate tetrahedron	745s	
500-550	δ (P–O^-), $(PO_4)^{3-}$	Deformed modes of P–O^-,$(PO_4)^{3-}$ group	518-565s	565s
487, 455	δ (P–O–P)	Bending unit is PO_4 tetrahedron	477s	-
330	δ -PO_2	Bending vibrations of phosphate polyhedral	418w	418w

Abbreviations: δ-deformation; *v*-stretching; s-symmetric; as-asymmetric, vs:very strong, s:strong, m:medium,w:weak, vw:very weak, sh:shoulder Refs. [24,25,26,27,28,29,30,31].

The characteristics features IR spectra of undoped powder compound on composition of 27.5SrO-27.5MgO-45P_2O_5 is the PO_2 asymmetric stretching vibration band at 1240 cm^{-1} $v_{as}(PO_2)$, the PO_2 symmetric stretching vibration band at 1190 cm^{-1} $v_s(PO_2)$, the v_{as} of POP groups at 958 cm^{-1}, the v_s of POP groups at 745 cm^{-1} and the deformation modes of P–O^-*(*PO_4^{3-}*)* groups at 565 and 477 cm^{-1}. This spectrum of undoped (Figure 2) shows a FT-IR pattern typical of metaphosphate such as $NaPO_3$ glass [26] and sodium copper phosphate [31]. The spectrum of the doped samples is almost following to the spectrum of the undoped and thereby the metaphosphate chains based on Q^2 and Q^1 groups are predominant in this composition.

The broad bands appear around 3447 cm^{-1} for doped and undoped sample. These bands can be accounted for by a different role of H_2O molecules in the structure. In particular, the atmospheric moisture is easily absorbed by the sample or by the pellet, causing the appearance of IR band belonging to H_2O molecules although the sample under investigation does not contain H_2O as unit in the network [3,12,17]. The bands located in the range 2700–2925 cm^{-1} are relatively weak and can be ascribed to the stretching vibrations of P–O–H group in different structural sites.

The band observed at 1322-1340 cm^{-1} is assigned to the characteristic stretching mode of the P=O bond. Several previous studies [32–37] have shown that the band corresponding to the stretching vibration of doubly bonded oxygen could be found in the frequency range 1230–1390 cm^{-1}. The band obviously becomes smaller indicating a decrease in the double bond character and in the effective force constant of the (P=O) bond as found in meta-phosphates with increasing dopant concentration (Eu_2O_3 content).

The band around 1240 cm^{-1} and 1190 cm^{-1} is assigned to asymmetric and symmetric stretching modes of the two non-bridging oxygen atoms bonded to phosphorus atoms, $v_{as}(PO_2)$ and $v_s(PO_2)$, in Q^2 units in the phosphate tetrahedral. Their amplitudes obviously decrease with increasing Eu_2O_3 content. This result indicates that the phosphate linkages are longer as the Eu_2O_3 incorporate into the metaphosphate structure and leading to decrease the relative content of the Q^2 units. Absorption band of PO_2

Corresponding Author: rbh@dfiz2.fs.utm.my

asymmetric stretching mode shifts from 1290 cm^{-1} in $NaPO_3$ glass [23,31] to ~1240 cm^{-1} in this studies.

The absorption bands near 1162 cm^{-1} have been assigned to $(P\text{-}O)^-$ groups and its amplitudes increase with increasing Eu_2O_3 content. It is suggested that the absorption bands due to M-O-P, with M = Sr/Mg, also locate at near 1100 cm^{-1}, and the relative content of these bonds increase with increasing Eu_2O_3 content leading to increased intensity of 1162 cm^{-1} band. Previous spectroscopic study [30] reported the asymmetric stretching vibration of the metaphosphate group, $\nu_{as}(PO_3)$, in the range 1080-1120 cm^{-1}. Therefore, in the present IR spectra, the $\nu_{as}(PO_3)$ could interfere with the band at 1162 cm^{-1}. The broadening character observed in the region 900–1100 cm^{-1} may lead to the assumption that the ν_{as} (PO_3) could also interfere in the range 1000– 1060 cm^{-1} [38].

The intensity of the band near 1023 cm^{-1}, which is assigned to (PO_3) end groups (Q^1), tends to decrease with increasing Eu_2O_3 content. The absorption bands near 958 and 721–745 cm^{-1} are assigned to the asymmetric and symmetric stretching modes of the (P-O-P) linkages, respectively. The asymmetric stretching band of (P-O-P) near 958 cm^{-1} initially shifts to higher frequencies as the amount of the Eu_2O_3 increases. The larger wave number of the (P-O-P) band is a result of the smaller (P-O-P) bond angle, which results from shorter phosphate linkages or smaller Sr/Mg cation size. The absorption bands near 518-562, 477 and 418 cm^{-1} are assigned to the stretching and deformation modes of $(PO_4)^{3-}$ groups (Q^0), respectively. The Q^1 and Q^0 groups decrease with increasing Eu_2O_3 content. These results indicate that the relative content of non-bridging oxygen $(P\text{-}O^-)$, which may be replaced by the formation of (M-O-P) bonds, decreases as the incorporation of the Eu_2O_3.

For doped sample, the intensities of PO_2 asymmetric stretching modes and of the ν_s of P–O–P bridges decrease as Eu_2O_3 content increases and the frequency of the ν_{as} of the PO_2 groups is shifted from 1270 to 1240 cm^{-1}. These changes in the spectra of the sample when Eu_2O_3 content increases are due to the decrease of the average phosphate chain length [39]. For Eu_2O_3 additions, the powder sample exhibit two bands in the frequency range 721–745 cm^{-1} which are attributed to the presence of two P–O–P bridges in metaphosphate chain based on $(P_2O_6^{2-})$ groups as shown in Figure 5a [40]. It is interesting to note that the sample exhibit only a single band at 740 cm^{-1} which is assigned to the P–O–P linkage in pyrophosphate group $P_2O_7^{4-}$ (Figure 3b) [40]. The band at 1240 cm^{-1} corresponding to $\nu_{as}(PO_2)$, smaller in the spectrum of the sample with increase Eu_2O_3, indicating that reduce chains group. These results are in accordance with the presence of pyrophosphate groups [37]. We conclude that when Eu_2O_3 is added to metaphosphate SrO-MgO-P_2O_5, the skeleton of $(P_2O_6^{2-})\infty$ chains is gradually broken into short phosphate groups such as $P_2O_7^{4-}$.

Corresponding Author: rbh@dfiz2.fs.utm.my

Solid State Science and Technology, Vol. 18, No 1 (2010) 288-301
ISSN 0128-7389

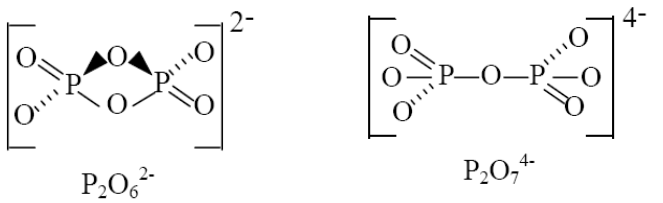

Figure 3: (a) Metaphosphate $(P_2O_6)^{2-}$ contains two P–O–P units. (b) Pyrophosphate $(P_2O_7)^{4-}$ contains only a single P–O–P bond [26].

Raman spectra of the powder phosphor samples 27.5SrO-27.5MgO-45P_2O_5:xEu_2O_3 ($1 \leq x \leq 5$ mol %) in the frequency range 400–1400 cm^{-1} are shown in Figure 4. The Raman spectrum of the sample contains sharper and better defined bands as expected for a crystallized material, compared to those for those glasses. The Raman bands are assigned based on the literature data on the wave number ranges related to the corresponding vibrations of the structural units in various glassy and crystalline phosphates [21–23]. The position and the relative intensity of each component of Raman spectra related to the vibrational mode of phosphate units were determined.

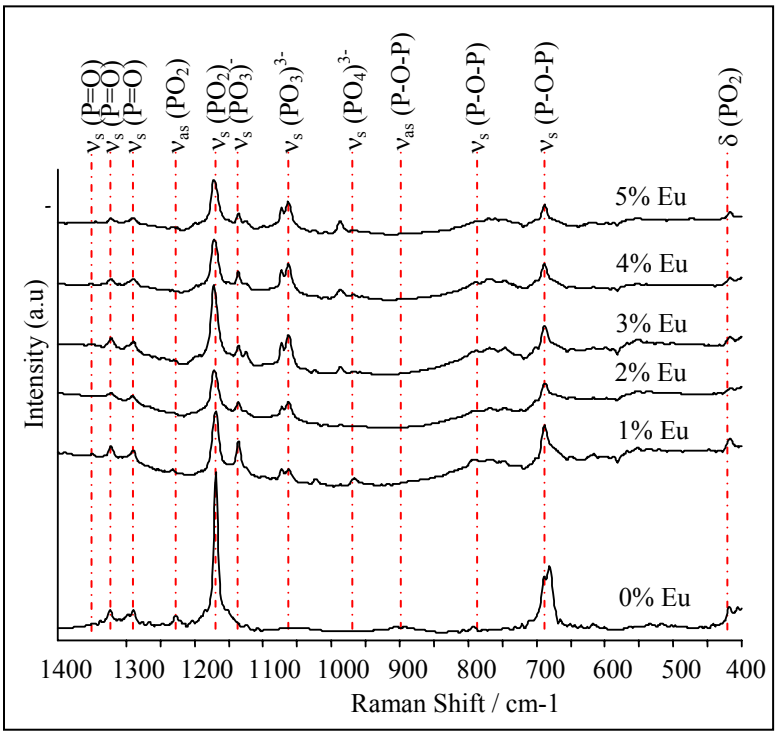

Figure 4: Raman spectra of 27.5SrO-27.5MgO-45P_2O_5:xEu_2O_3 ($1 \leq x \leq 5$mol%) powder phosphor sample.

Corresponding Author: rbh@dfiz2.fs.utm.my

The Raman spectrum of undoped sample, consists of very sharp lines at 1322, 1240, 1171, 688 and 420 cm^{-1}. The bands, at 688, 1171 and 1240 cm^{-1}, which are assigned to metaphosphate chain structures, decrease little bit with increasing Eu_2O_3 content. At the doping powder sample, three Raman lines, at 967, 1062 and 1136 cm^{-1} are appearing in the spectra. Also, with increasing Eu content, the bands near 1171 and 688 cm^{-1} have decreases in the spectrum and the bands near 1136, 1062 and 967 cm^{-1} are predominate, that is, the bands characteristic of the pyrophosphate dimer $(P_2O_7)^{4-}$ and orthophosphate monomer $(PO_4)^{3-}$ species increased.

The band near 1322 cm^{-1} is assigned to the symmetric stretching mode of terminal oxygen (P=O). With increase Eu_2O_3 content, the (P=O) stretching mode bands becomes smaller indicating a decrease in the double bond character and in the effective force constant of the (P-O) bond as found in ultraphosphates. The lines at 1240 and 1171 cm^{-1}, respectively, correspond to the asymmetric and symmetric stretching modes of the two non-bridging oxygen atoms bonded to phosphorus atoms (PO_2) [20]. These three bands (1240, 1170 and 688) are in agreement with the value of 1267, 1165 and 689 cm^{-1} reported by Nelson et. al for metaphosphate $NaPO_3$ glass [33] and sodium orthophosphate [18], suggesting that the structure of this composition consists essentially of a long phosphate chains based on PO^{3-} units.

With increasing of doping Eu_2O_3 in samples, bands at 1136 and 1062 cm^{-1} are related to the symmetric stretching mode of $P_2O_7^{4-}$ units (Q^1 tetrahedral), which indicate a present of pyrophosphate groups in the network in these sample, and symmetric terminal $(PO_3)^-$ symmetric groups in Q^1 pyrophosphates appeared in Raman spectra. Such an evolution of $(PO_3)^-$ the Raman spectra is similar to that reported for the lead phosphate glasses [19]. These results agree with the IR spectra where the pyrophosphate, $P_2O_7^{4-}$ along with the orthophosphate, $(PO_4)^{3-}$ units are dominant in the structures of samples. The terminal stretching modes of $P_2O_7^{4-}$ ions usually occur in the region 1250-975 cm^{-1} [23]. When the Q^1 tetrahedrons are the majority species in phosphate sample, a strong and broad band appears at 1080 cm^{-1} in the Raman spectrum [22]. On the other hand, the dominance of Q^2 species causes a band at 1200 cm^{-1} [7]. The verification of these conclusions will be possible when our efforts on the field of the single crystal synthesis for this compound will be successful.

Similar values (~1060 and 730 cm^{-1}) have been reported by Stranford et al. [23] for the P–O–P and PO_3 symmetric stretching modes of α-$Zn_2P_2O_7$. There are also some traces of orthophosphate groups $(PO_4)^{3-}$ as indicated by the band near 967 cm^{-1}. The present of the isolated $[PO_4]^{3-}$ anion is characterized by four tetrahedron internal modes namely by two stretching modes at 1072 cm^{-1} and 967 cm^{-1} and two bending modes at ~565 cm^{-1}.

The intense band at 1078 cm^{-1} has been attributed to the symmetric stretching vibration of pyrophosphate, $(P_2O_7)^{4-}$ units present in crystalline $Sr_2P_2O_7$ [19], whereas the band at 944 cm^{-1} corresponds to the symmetric stretching of the $(PO_4)^{3-}$ groups in β-$MgO(PO_3)_2$. The presence of bands at 967 cm^{-1} in the spectrum indicates isolated

Corresponding Author: rbh@dfiz2.fs.utm.my

$(PO_4)^{3-}$ group or Q^0 phosphate units. The frequency of this band, assigned to the symmetric stretching mode of non-bridging oxygen in orthophosphate groups, is close to the value of 945 cm^{-1} for sodium orthophosphates reported by Nelson et al. [22]. The bands at 688 cm^{-1} are attributed to the bridging $(P–O–P)_{sym}$ oxygen atoms in Q^2 metaphosphate groups respectively. The band at 730 cm^{-1} is attributed to the bridging $(P–O–P)_{sym}$ oxygen atoms in Q^1 phosphate groups, respectively [14, 17]. The bands at 418 cm^{-1} are assigned to the bending vibrations.

By comparing the Raman spectrum with the IR spectrum for powder samples, bands located in similar positions can be observed, which is characteristic of low symmetry materials [27]. For the crystalline sample, the position of most Raman and IR bands does not coincide indicating a higher symmetry (the selection rules for IR and Raman spectroscopy are not the same) [28]. The presence of Q^1 species detected by the Raman spectroscopy is confirmed in the IR spectrum, where the IR bands around 958 and 721-745 cm^{-1} correspond to symmetrical and asymmetrical P–O–P stretching modes, respectively [24].

It is generally admitted that the symmetry stretching vibrations (ν_sPOP) in chain metaphosphate occur in the range close to 700 cm^{-1} as strong Raman lines and weak IR bands. The anti-symmetric modes (ν_{as}POP) are located around 900–800 cm^{-1} and give rise to strong IR bands and weak Raman lines. In the low-frequency region below 650cm^{-1}, it is very difficult to distinguish the anti-symmetric (δ_{as}) and symmetric (δ_s) bending modes $(PO_2)^-$ species and (δPOP) bending. Moreover, these modes overlay with external modes. All of these bands are characteristic of infinite chain of PO_4 tetrahedra bound by bridging oxygen. A comparison of the Raman and IR positions of bands (see Table 1) shows that the majority of them are not coincident; this fact is in agreement with the centrosymmetric structure of $SrMgP_2O_5$.

It is well known that the structure of phosphate is strongly dependent on the O/P ratio of their composition [19]. With increasing O/P ratio, the phosphate network becomes more depolymerized and the ultraphosphate structure composed of cross-linked Q^3 units (O/P = 2.5) changes to the chain-like metaphosphate structure made up of Q^2 units (O/P = 3.0) to the pyrophosphate, Q^1, structure (O/P = 3.5) and finally to the orthophosphate structure consisting of isolated Q^0 units (O/P = 4.0). In the composition in the present studies, the O/P ratio is nearly constant at ~3.1, so the network structure is expected to be dominated by metaphosphate, Q^2 and pyrophosphate, Q^1 groups. Nevertheless, the basic phosphate network in powder sample consists of pyrophosphate units, $P_2O_7^{4-}$ since the Raman spectra, Figure 4, revealed the largest intensity of the bands at 1136 and 1062 as well as 987 cm^{-1}, i.e, the phosphate network also contains a small fraction of orthophosphate, Q^0 units. Similar behavior was found in zinc and iron phosphate glasses [17]. The presence of a certain amount of isolated, $(PO_4)^{3-}$, orthophosphate groups and $–O–(PO_2)^-$ species (the monomer of the polymeric metaphosphate chain) along with the $P_2O_7^{4-}$ pyrophosphate groups in in these powder sample due to an equilibrium between the pyrophosphate units and the products of their disproportion in powder according to the following [17]:

Corresponding Author: rbh@dfiz2.fs.utm.my

$$(PO_3)^{2-} - O - (PO_3)^{2-} \leftrightarrow (PO_4)^{3-} + - O - (PO_2)^{-} \quad (1)$$

Such equilibrium is also believed to explain the small amount of the metaphosphate chains and isolated orthophosphate units in the powder sample.

CONCLUSIONS

Infrared and Raman spectroscopy have been used to determine the structure of 27.5SrO-27.5MgO-45P_2O_5:*x*Eu_2O_3 ($1 \leq x \leq 5$) powder phosphor sample. The composition of alkali earth ions, (Mg^{2+} and Sr^{2+}) produce significant changes of the phosphate structure from a three-dimensional random network,Q^3 to long or very short chains of PO_4 tetrahedral. SrO and MgO breaks up the structure of $(PO_3)\infty$ chains in the metaphosphate composition into the smaller groups $P_2O_7^{4-}$. The addition of $1 \leq x \leq 5$ mol% Eu_2O_3 produces a significant effect on local structure host phosphor which has been detected clearly by Raman comparable IR cannot detected. The use of complementary techniques Raman and infrared (IR) spectroscopy has proven to be an efficient examination way of the local structure, in general and of the phosphate structure, in particular. The vibrational properties of studied materials strongly depend on the type of phosphate. The position and shape of their IR and Raman spectra give a characteristic pattern that allows defining the type and structure of the material. The shape of Raman spectra of the studied powder compound is influenced by the presence of dopant Eu_2O_3. The phosphate chain in metaposphate is depolymerized with the increasing of Eu_2O_3 so in consequence its characteristic bands strongly increase in intensity. The basic structure unit in phosphate network in powder sample studies consists of pyrophosphate units, $P_2O_7^{4-}$ and also contains some metaphosphate and orthophosphate units. Besides that, structural studies can also investigating the influences of water with host networks, have utilized both Infrared (IR) spectroscopy and Raman spectroscopy to determine distinct proton environments in powder sample.

ACKNOWLEDGMENTS

This report is based upon work supported by the Ministry of Science Technology and Innovation (MOSTI) under research grant Project Number: 03-01-06-SF0053. Acknowledgment is made to Ibnu Sina Institute, Department of Chemistry Faculty of Science UTM and Faculty of Mechanical UTM for providing the Raman, FT-IR spectroscopy and XRD measurement facilities. We also thank an anonymous reviewer for helpful comments.

REFERENCES

[1]. G. Blasse, B.C. Grabmaier, Lumin. Mater. **115** (1994) 140.
[2]. S. Shionoya, W.M. Yen, Phosphor Handbook, vol. **391**, 1999.
[3]. R. Hussin, D. Holland, R. Dupree, J. Non-Cryst. Solids **298** (2002)32.
[4]. C.M. Shaw, J.E. Shelby, J. Am. Ceram. Soc. **71** (1988) C252.
[5]. R.K. Brow, R.J. Kirkpatrick, G.L. Turner, J. Am. Ceram. Soc. 76 (1990) 293.
[6]. Y.B. Peng, D.E. Day, Glass Technol. **32** (1991) 166.
[7]. I.W. Donald, J. Mater. Sci. **28** (1993) 2841.

Corresponding Author: rbh@dfiz2.fs.utm.my

[8]. M.R. Reidmeyer, D.E. Day, G.J. Long, J. Non-Cryst. Solids **181** (1995) 201.
[9]. M. Karabulut, G.K. Marasinghe, G.S. Ray, D.E. Day, O. Ozturk, G.D. Waddil, J. Non-Cryst. Solids **249** (1999) 106.
[10]. G.N. Greaves, S.J. Gurman, L.F. Gladden, C.A. Spence, P. Cox, B.C.Sales, L.A. Boatner, R.N. Jenkins, Phil. Mag. B **58** (1988) 271.
[11]. S.T. Reis, M. Karabulut, D.E. Day, J. Non-Cryst. Solids **292** (2001)150.
[12]. R. Sahar, A. Wahab M.A. Hussein, R. Hussin, J. Non-Cryst. Solids, Vol. **353** 11-12(2007)1134.
[13]. Shaharudin Ali, Rosli Hussin, M.Rahim Sahar and Mustamam A. Karim, Jornal solid state science and Technology, Vol. **6**, 2000.
[14]. Agus S.B., Shaharudin B.A., Rosli B.H, M.R. Sahar and M.A.A. Sidek, Jornal solid state science and Technology, Vol. **8** No. 1&2 (2001)149.
[15]. A.M.A. Hussein, R. Hussin and M.R. Sahar, Journal Solid State Science and Technology, Vol. **8** No. 1&2 (2001) 1
[16]. S. Budi, R. Hussin, M.R. Sahar, and M.M.A. Karim, Journal Solid State Science and Technology, Vol. **8** No. 1&2 (2001) 9-18.
[17]. R.Hussin, A.S. Musdalilah., A. Nur Shahira, A. Mutia Suhaibah, A. Suhailah, A.F. Siti Aishah, H. Sinin and M.Y. Mohd Nor, Journal of Fundamental Science 2008 (accepted for published).
[18]. J.R. van Wazer, Phosphorus and its Compounds vol.**1**, Interscience, New York, 1958.
[19]. R.K. Brow, J. Non-Cryst. Solids **263** (2000) 1.
[20]. R.K. Brow, R.J. Kirkpatrick, G.L. Turner, J. Non-Cryst. Solids **116** (1990) 39.
[21]. X. Fang, C.S. Ray, A. Mogus-Milankovic and D.E. Day, J. Non-Cryst. Solids **283** (2001) 162.
[22]. C. Nelson and D.R. Tallant, Phys. Chem. Glasses **26** (1985) 119.
[23]. E. Efimov, J. Non-Cryst. Solids **209** (1997) 209.
[24]. P.Y. Shih, S.W. Yung, T.S. Chin, Journal of Non-Crystalline Solids **244** (1999) 211-222
[25]. D.E. Corbridge, J. Appl. Chem. **6** (1956) 456.
[26]. L. Montagne, G. Palavit, G. Mairesse, Phys. Chem. Glasses **37** (1996) 206.
[27]. K. Meyer, J. Non-Cryst. Solids **209** (1997) 227.
[28]. J.J. Hudgens, S.W. Martin, J. Am. Ceram. Soc. **76** (1993)1691.
[29]. A. Mogusˇ-Milankovic, A. Sˇ antic, S.T. Reis, K. Furic and D.E. Day, Journal of Non-Crystalline Solids **351** (2005) 3246–3258.
[30]. R.K. Brow, D.R. Tallant, S.T. Myers, C.C. Phifer, J. Non-Cryst. Solids **191** (1995) 45.
[31]. A. Chahine, M. Et-tabirou, J.L. Pascal, Materials Letters **58** (2004) 2776– 2780
[32]. S.M. Abo-Naf, N.A. Ghoneim, H.A. El-Batal, J. Mater. Sci.: Mater. Electron. **15** (2004) 273.
[33]. Md. Rafiqul Ahsan, M. Golam Mortuza, J. Non-Cryst. Solids **351** (2005) 2333.
[34]. M. Hafid, T. Jermoumi, N. Toreis, T. Ghailassi, Mater. Lett. **56** (2002) 486.
[35]. T. Jermoumi, S. Hassan, M. Hafid, Vib. Spectrosc. **32** (2003) 207.
[36]. E. Metwalli, M. Karabulut, D.L. Sidebottom, M.M. Morsi, R.K. Brow, J. Non-Cryst. Solids **344** (2004) 128.

Corresponding Author: rbh@dfiz2.fs.utm.my

[37]. H. Doweidar, Y.M. Moustafa, K. El-Egili, I. Abbas, Vib. Spectrosc. **37** (2005) 91.
[38]. M. Abid, M. Et-tabirou, M. Hafid, Mater. Res. Bull. **36** (2001) 407
[39]. D.E.C. Corbridge, J.E. Lowe, J. Chem. Soc. Part I (1954) 493.
[40]. M.A. Salim, G.D. Khattak, M. SakhawatHussain, J. Non-Cryst. Solids **185** (1995) 101.

Corresponding Author: rbh@dfiz2.fs.utm.my